3828 *Biochemistry* **2009,** *48,* 3828–3837
DOI:10.1021/bi900212j

BIOCHEMISTRY
including biophysical chemistry & molecular biology
Current Topic

Structure and Mechanism of Protein Stability Sensors: Chaperone Activity of Small Heat Shock Proteins[†]

Hassane S. Mchaourab,* Jared A. Godar, and Phoebe L. Stewart

Department of Molecular Physiology and Biophysics, Vanderbilt University, Nashville, Tennessee 37232

Received February 9, 2009. Revised Manuscript Received March 24, 2009

ABSTRACT: Small heat shock proteins (sHSP) make up a remarkably diverse group of molecular chaperones possessing a degree of structural plasticity unparalleled in other protein superfamilies. In the absence of chemical energy input, these stability sensors can sensitively recognize and bind destabilized proteins, even in the absence of gross misfolding. Cellular conditions regulate affinity toward client proteins, allowing tightly controlled switching and tuning of sHSP chaperone capacity. Perturbations of this regulation, through chemical modification or mutation, directly lead to a variety of disease states. This review explores the structural basis of sHSP oligomeric flexibility and the corresponding functional consequences in the context of a model describing sHSP activity with a set of three coupled thermodynamic equilibria. As current research illuminates many novel physiological roles for sHSP outside of their traditional duties as molecular chaperones, such a conceptual framework provides a sound foundation for describing these emerging functions in physiological and pathological processes.

Following their emergence from the ribosomes, newly synthesized proteins navigate an energy hypersurface replete with conformational dead ends and punctuated by kinetic detours to reach the native biologically active conformation (*1*, *2*). Along this journey, hydrophobic stretches of residues are progressively shielded from solvent, generally through packing in the protein core or at interfaces. Long transit times through local energy minima leave partially folded proteins with exposed hydrophobic surfaces vulnerable to the dead-end pitfalls of aggregation (*3*). Successful arrival at the global energy minimum does not eliminate the danger of aggregation. The marginal stability of the folded states implies that proteins constantly sample partially unfolded conformations, exposing hydrophobic residues in the crowded cellular environment (*4*, *5*). The rates of these equilibrium transitions increase under stress conditions which may lead to loss of protein solubility. Aggregation wastes cell resources, and protein aggregation diseases can be infectious, dementing, and even fatal (*6*). Nature has devised multiple and redundant responses to inhibit protein aggregation or dispose of protein aggregates. One such response involves expression of multiple families of heat shock proteins that function as molecular chaperones each specialized for dealing with a different aspect of protein folding and stability (*7*−*15*). Some chaperones guide proteins along their journey to the native state, avoiding local energy minima or rescuing them from such detours. Other chaperones buffer the rapid increase in the level of aggregation-prone, misfolded proteins that inevitably follows environmental perturbations.

Although heat shock proteins have broad specificity for non-native proteins, their functions vary in mechanistic complexity, ranging from passive binding for preventing aggregation to energy-dependent facilitated folding of specific classes of proteins (*7*−*15*). The small heat shock proteins (sHSP)[1] make up a ubiquitous family of passive, energy-independent chaperones (*16*−*19*). This superfamily consists of heat-inducible proteins with a molecular mass between 12 and 40 kDa per subunit possessing a conserved stretch of ∼100 residues termed the α-crystallin domain (Figure 1A). This domain is flanked at the N-terminal side by a hydrophobic region that varies in sequence and length and at the C-terminal side by a short tail or extension with a conserved sequence motif. Invariably, sHSP subunits assemble into oligomeric structures with a broad spectrum of sizes, symmetries, and structural order, which relate to their function and modes of interaction with unfolded or destabilized proteins (*18*−*20*). Interest in sHSP has been stimulated by the identification of their roles in critical

[†]This work was supported by the National Eye Institute, National Institutes of Health Grants R01-EY12683 and R01-EY12018 to H.S.M., and Molecular Biophysics Training Grant T32GM008320 to J.A.G.

*To whom correspondence should be addressed: Vanderbilt University, 741 Light Hall, Nashville, TN 37232-0615. Phone: (615) 322-3307. Fax: (615) 322-7236. E-mail: hassane.mchaourab@vanderbilt.edu.

[1]Abbreviations: sHSP, small heat shock protein(s); MJ, *Methanocaldococcus jannaschii*; Ta, *Triticum aestivum*; FRET, Förster resonance energy transfer; EPR, electron paramagnetic resonance; CryoEM, cryo-electron microscopy; T4L, T4 lysozyme; MDH, malate dehydrogenase.

 Published on Web 3/26/2009

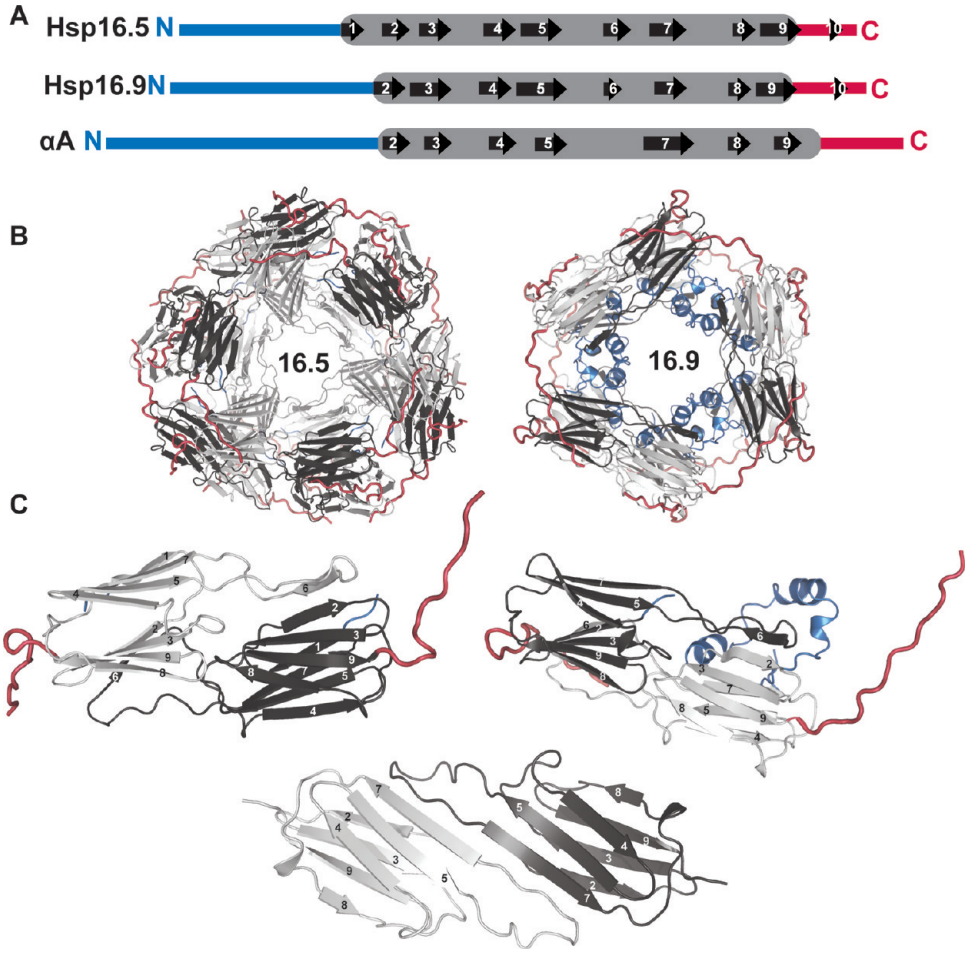

FIGURE 1: Small heat shock protein architecture. (A) Schematic representation of Hsp16.5, Hsp16.9, and αA-crystallin drawn to scale depicting the α-crystallin domain (gray) flanked by N-terminal (blue) and C-terminal (red) extensions with β-strands as black arrows. (B) Quaternary structures of MJ Hsp16.5 spherical 24-mer (left) and the dodecameric double disk of wheat Hsp16.9 (right) with N- and C-terminal extensions colored as in panel A and the asymmetric α-crystallin domains of each dimer shaded in light and dark gray. (C) Hsp dimers with strands numbered as in panel A. αA-Crystallin depicted as modeled from EPR distance analysis (*55*). Note domain-swapped strand 6 of Hsp16.5 and -16.9 and its absence in αA-crystallin.

cellular processes such as aging (*21*) and apoptosis (*22*−*24*), as well as by the discovery of mutants associated with human diseases, including cataracts (*25*, *26*) and cardiomyopathies (*27*). Over the past two decades, genetic, biochemical, and structural studies have provided a wealth of information about the physiological roles and functional mechanisms of sHSP. In *Caenorhabditis elegans*, sHSP promote longevity and couple the normal aging process to age-related diseases such as polyglutamine expansion protein aggregation (*21*). sHSP may provide a therapeutic advantage for neurodegenerative diseases, such as amyotrophic lateral sclerosis and multiple sclerosis (*28*−*30*), with which they are associated. Studies using intact vascular smooth muscle demonstrate key roles for sHSP in regulation of smooth muscle tone and active participation in kinase signaling cascades (*31*). Discovery and characterization of additional physiological contributions continue to expand the importance of sHSP beyond their traditional chaperone duties. This review focuses on structural and mechanistic aspects of sHSP, including the determinants of their oligomeric assembly, their mechanism of sensing non-native proteins, and the structural basis of regulation of sHSP chaperone activity.

Nowhere is protein folding and stability more readily associated with disease than in the ocular lens (*32*). The "wear and tear" of lens aging is recorded at the molecular level through accumulated modifications to the crystallins, the major protein components of fiber cells (*33*−*35*). In the absence of protein turnover in the lens, these modifications lead to a progressive loss of crystallin stability and solubility, as well as altered protein−protein interactions, all of which compromise lens transparency and refractivity and may lead to cataracts (*33*, *36*). Roughly 35% of a lens fiber cell by weight consists of αA- and αB-crystallin, a sHSP presumed to inhibit the aggregation of damaged and destabilized proteins (*37*, *38*). α-Crystallin-deficient mice have smaller lenses that develop opacity shortly after birth (*39*). Furthermore, a number of point mutations in human α-crystallin genes have been associated with hereditary cataracts (*25*, *26*, *40*, *41*), confirming the critical role of this sHSP in maintaining lens transparency. α-Crystallins are the most studied sHSP, and the lens provides a unique model system for linking in vitro mechanistic analysis to phenotypic models (*42*, *43*).

STRUCTURAL FRAMEWORK

sHSP assemble into remarkably versatile oligomers with a level of divergence unparalleled in other protein superfamilies. Not only do sHSP oligomers display wide varia-

tions in the number of subunits and their packing symmetry, but they also show substantially different degrees of order and dispersity (*20*). The spectrum ranges from highly symmetric and monodisperse assemblies (*44*) to polydisperse oligomers actively exchanging subunits (*45*, *46*). Although dynamics and heterogeneity hinder high-resolution structural analysis of a class of sHSP, the determinants of variable architecture and its mechanistic roles have emerged from visualization of oligomers (*20*, *44*, *47*), characterization of their dynamics by spectroscopic approaches (*48*, *49*), and the correlation between oligomer dynamics and substrate binding (*50*−*54*). On a more general level, the analysis of sHSP assemblies is providing unique insights into the role of dynamics in protein function and identifying new motifs of structural plasticity.

α-*Crystallin domain building block*. Consistent with its conserved sequence, the α-crystallin domain is a common structural module that plays a central role in sHSP oligomeric structure across the evolutionary spectrum. α-Crystallin domain dimers are the building blocks for the two ordered sHSP oligomers with known high-resolution structures, *Methanocaldococcus jannashii* (MJ) Hsp16.5 (*44*) and *Triticum aestivum* (Ta) Hsp16.9 (*47*) (Figure 1B). Each α-crystallin domain monomer has an immunoglobulin core fold consisting of seven *β*-strands arranged in two antiparallel sheets (Figure 1C). The two monomers interact via an extended loop, and the dimer is stabilized by swapping of a peripheral *β*-strand (*β*6) which interacts with the edge of the *β*-sandwich in the symmetry-related subunit. While this seven-stranded core fold is conserved in mammalian sHSP αA-crystallin (*55*), sequence modifications, including deletion of the swapped strand, lead to a different dimerization interface (*56*−*58*). In αA-crystallin and Hsp27, the two monomers are related by a 2-fold symmetry axis located near the N-terminal end of strand 7 (Figure 1C). A similar geometry for the αB-crystallin dimer was deduced from small-angle X-ray scattering (*59*), suggesting that the altered monomer−monomer packing is conserved among mammalian sHSP and thus may have important consequences for their oligomeric structures. Recent NMR analysis of a truncated construct of αB-crystallin consisting of its α-crystallin domain identified six *β*-strands (*60*). The sequence corresponding to *β*2 of αA-crystallin appeared to be unstructured, possibly reflecting an artifact of truncation or more interestingly structural differences between αA- and αB-crystallin. Although the authors suggest their data in the region of strand 7 differ from the EPR model, close inspection of their sequence-specific secondary structure assignment suggests the perceived deviation of one residue (F113) is simply an artifact of sequence alignment.

Packing of the α-*Crystallin dimers*. In the native Hsp16.5 and Hsp16.9 oligomers, α-crystallin domain dimers are held together by the C-terminal tail of one sHSP monomer binding in a hydrophobic groove at the C-terminal edge of the *β*-sandwich contributed by another dimer (Figure 1B). The sequence elements involved in this interaction are conserved across the superfamily, suggesting this dimer−dimer connection is a core structural motif (*16*, *17*). Indeed, EM analysis of Acr1,

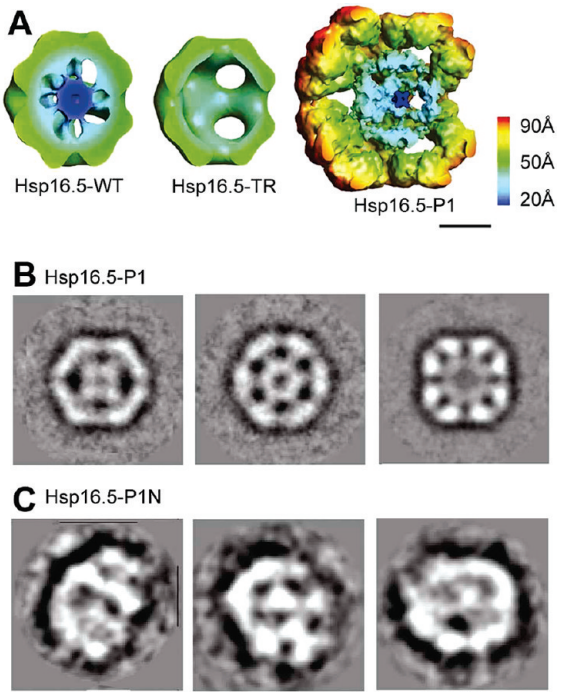

FIGURE 2: CryoEM structural information for wild-type (WT) Hsp16.5 and engineered variants. (A) Three-dimensional CryoEM reconstructions of WT Hsp16.5, Hsp16.5-TR, and Hsp16.5-P1 (left to right) shown cropped in half and radially color-coded (10 Å radius, blue; 90 Å radius, red) with a 50 Å scale bar. (B) Three selected CryoEM class sum images of Hsp16.5-P1 displaying nearly perfect 2-, 3-, and 4-fold symmetry (left to right). (C) Three CryoEM class sum images of Hsp16.5-P1N selected to represent the diversity and lack of symmetry in the majority of the class sum images. Adapted with permission from ref *70*. Copyright 2009 The American Society for Biochemistry and Molecular Biology.

one of two *Mycobacterium tuberculosis* sHSP, suggests a similar role for this sequence in the assembly of a dodecameric oligomer (*61*). A hinge linking the C-terminal tail to the α-crystallin domain provides the flexibility necessary to generate oligomer diversity while preserving the dimer−dimer interface. The importance of this motif is highlighted by comparison of Hsp16.5 and Hsp16.9 oligomeric structures (*44*, *47*). Despite possessing the same conserved α-crystallin domain fold and a similar dimeric building block, Hsp16.5 assembles into a spherical oligomer of 24 subunits with octahedral symmetry, while Hsp16.9 subunits assemble into two stacked hexameric disks. Formation of these distinct assemblies is facilitated by a 30° change in the orientation of the C-terminal extensions relative to the α-crystallin domain, allowing two different dimer packing arrangements within an Hsp16.9 oligomer. The Hsp16.5 and Hsp16.9 oligomers are also differentially stabilized by their respective N-terminal regions (*47*). The N-termini of Hsp16.9 monomers interact through an unusual helix knotting that intertwines monomers from the two rings (Figure 1B). In contrast, truncation of Hsp16.5 N-termini does not change the size or symmetry of the oligomer (*62*) (Figure 2A).

Oligomeric structure: from ordered symmetric to polydisperse. Mammalian sHSP, in contrast, form dynamic polydisperse oligomers rather than symmetrical assemblies (*46*,*50*,*63*−*65*). CryoEM analysis of α-crystallins and Hsp27 reveals particles of different sizes with little if any

evidence of symmetry. This heterogeneity hinders high-resolution analyses of mammalian sHSP, although some of their structural features have been deduced from systematic application of spin labeling and EPR spectroscopy (*57*). While the α-crystallin domain fold appears to be preserved in the α-crystallins and Hsp27, the N-terminal region evolved to control the global packing arrangement, oligomer dynamics, and order (*45*, *57*, *66*). Mammalian sHSP exchange subunits in a process that involves equilibrium dissociation and reassociation of dimers and/or monomers. In a classic FRET experiment, Bova et al. measured the rate constant of subunit exchange between oligomers of α-crystallin and demonstrated that these rates are orders of magnitude faster than expected on the basis of unfolding kinetics (*45*, *64*). Truncation of the N-terminal region leads to dissociation of αA-crystallin into dimers and tetramers that do not exchange subunits (*45*, *57*, *66*, *67*). Similarly, yeast Hsp26 oligomerization depends on its N-terminal domain (*68*). Subunit exchange is not unique to polydisperse sHSP; the ordered TaHsp16.9 exchanges subunits with PsHsp18.1 under native conditions (*47*, *69*). Compelling evidence suggests that equilibrium dissociation is a mechanism of sHSP activation (*51*, *54*).

Determinants of SHSP oligomer plasticity. The interplay among the three sequence modules (N-terminal region, α-crystallin domain, and C-terminal extension) in the transition from ordered symmetrical to polydisperse assemblies was experimentally tested through structural and functional characterization of engineered Hsp16.5 oligomers (*70*). The transposition of an N-terminal sequence element from the polydisperse human Hsp27 into the monodisperse Hsp16.5 results in either a symmetric expansion or transformation to polydisperse assemblies (Figure 2). A hybrid approach combining spin labeling EPR and CryoEM revealed that the expanded symmetric oligomer, hereafter termed Hsp16.5-P1, consists of 48 subunits compared to 24 for the WT (Figure 3). In the Hsp16.5-P1 structure, the two monomers in the dimeric building block are not equivalent, primarily due to a change in the orientation of the C-terminal extension similar to the hinge mechanism observed in Hsp16.9 (Figure 3C). This rearrangement leads to a novel 4-fold window ~45 Å in diameter, which is not present in the WT oligomer. The four dimers around the 4-fold window are tethered by C-terminal extensions in the modified orientation. A polydisperse form of Hsp16.5, termed Hsp16.5-P1N, is created when the same Hsp27 sequence element is inserted at a different site within the Hsp16.5 N-terminal region (Figure 2C) (*70*).

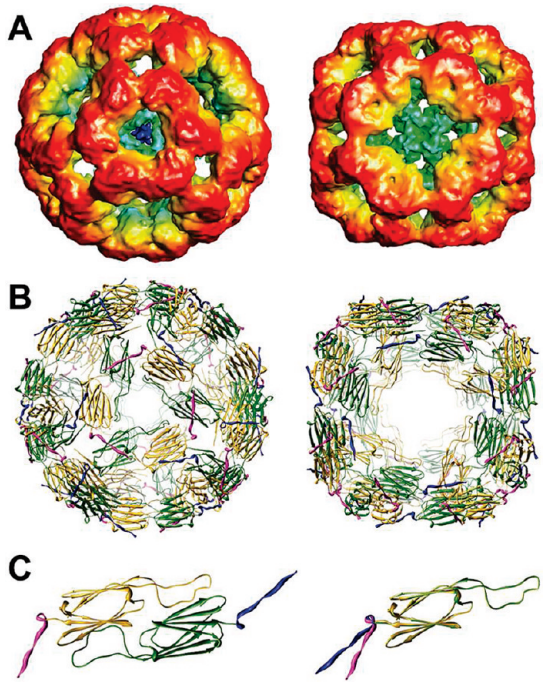

FIGURE 3: CryoEM structure and pseudoatomic model of Hsp16.5-P1. (A) CryoEM structure at 10 Å resolution aligned along the 3- and 4-fold symmetry axes, from left to right. The radial color coding is the same as in Figure 2. (B) Pseudoatomic model of Hsp16.5-P1 containing 48 α-crystallin domain monomers as viewed along the 3- and 4-fold symmetry axes. The independent monomer positions are colored either gold with magenta C-terminal tails (chain A) or green with blue C-terminal tails (chain B). (C) α-Crystallin domain dimer from the pseudoatomic model showing the two different C-terminal tail conformations (left). Superimposition of the two monomers within the dimer (right) shows the deviation in the angle of the C-terminal tail relative to the α-crystallin domain. This angle deviation allows the dimer to accommodate packing around either the 3- or 4-fold openings of the assembly. Adapted with permission from ref *70*. Copyright 2009 The American Society for Biochemistry and Molecular Biology.

The results of this protein engineering experiment are consistent with the notion that modification of the N-terminal region, a distinctive hallmark in sHSP evolution, affects the overall oligomeric order and symmetry of the assembly. Changes in the N-terminal region are propagated to the dimer−dimer interface and can lead to expanded symmetrical assemblies or to irregular and polydisperse assemblies. Creation of polydisperse Hsp16.5-P1N also resolves the conundrum of how an irregular assembly can form from a folded and stable structural building block, in this case, the conserved α-crystallin domain dimer. A dimer−dimer interface with minimal contacts and a flexible C-terminal hinge provides this plasticity by adopting different angles to accommodate multiple higher-order oligomers.

Both the expanded and polydisperse engineered forms of Hsp16.5 have increased affinities for destabilized substrates relative to WT Hsp16.5, supporting the direct coupling between oligomeric structure and chaperone activity (*70*). In contrast, deletion of the N-terminal region significantly reduces substrate affinity, suggesting this buried sequence is likely critical for substrate binding.

MECHANISM OF SHSP CHAPERONE ACTIVITY

While all molecular chaperones bind proteins in non-native states, they differ in their mechanism of substrate recognition, as well as in the conformation and fate of the bound substrate (*11*). Despite a critical role in conferring thermotolerance (*18*), the involvement of sHSP in cellular protein refolding is less clear. One current model postulates that under conditions of extreme stress sHSP provide an energy-independent mechanism for buffering the increase in the level of non-native proteins (*71*, *72*). sHSP chaperone activity does not require the input of ATP energy, and the binding capacity can reach one substrate protein per sHSP subunit of equal molecular mass. Thus, sHSP can be a major contributor to the chaperone capacity of a cell.

Scheme 1: Coupled Equilibria Describing the Minimalist Model

$$N \rightleftharpoons I_1 \rightleftharpoons \ldots \rightleftharpoons I_i \rightleftharpoons U \quad (1)$$

$$sHSP \rightleftharpoons (sHSP)_a \quad (2)$$

$$(sHSP)_a + \begin{pmatrix} I_1 \\ U \end{pmatrix} \rightleftharpoons \begin{pmatrix} C_1 \\ C_u \end{pmatrix} \quad (3)$$

Although sHSP−substrate complexes are stable (*71*, *72*), release and refolding of the bound substrate can be accomplished in vitro through interactions with Hsp70. Cooperative cellular chaperone networks have been proposed to play a central role in protein folding and in stress response (*73*).

Initial characterization of sHSP chaperone activity relied primarily on observation of the suppression of light scattering by aggregating proteins. In brief, substrate proteins are exposed to conditions that promote unfolding, subsequent aggregation, and precipitation. Chaperone efficiency is defined empirically as the reduction in light scattering by the substrate in the presence of the chaperone. These convenient and experimentally simple assays confirmed the broad specificity of sHSP and defined the basic characteristics of their interactions with substrate proteins (*18*). However, determination of binding parameters and structural analysis of the interaction complex are hindered by the nonequilibrium nature of these aggregation-based assays. The experimental observable, change in light scattering, reflects the kinetic competition between self-association of the substrate and binding to the chaperone (*49*). Furthermore, these assays employ strongly denaturing conditions resulting in a conformationally heterogeneous ensemble of bound substrates that is not readily amenable to structural analysis. These extreme conditions may also compromise the structural and functional integrity of the chaperone. From a physiological perspective, mutations or post-translational modifications can shift the folding equilibrium toward non-native states but often do not lead to a positive ΔG_{unf} characteristic of most aggregation assays. Thus, such assays do not recapitulate the predominant interactions of chaperones within the cellular environment that must precede nucleation of aggregation.

Mchaourab et al. (*74*) demonstrated that sHSP detect the increased excursions of destabilized proteins toward aggregation-prone non-native states under conditions that favor the native state in the absence of substrate aggregation. Progressive reduction in the folding equilibrium constant of T4 lysozyme (T4L) via site-directed mutagenesis triggers the formation of a stable complex with sHSP, although the T4L folded state is favored by 3−7 kcal/mol as calculated from the experimentally determined ΔG_{unf}. These studies took advantage of the thorough analysis of T4L folding and stability that yielded a library of thermodynamically destabilized, site-directed mutants with known crystal structures (*75*, *76*). Formation of a complex between substrate and sHSP was initially detected by altered spectroscopic signatures of spin or fluorescence labels (*74*, *77*, *78*) attached at a unique, solvent-exposed cysteine in the substrate. Recently, a new label-free approach has been introduced to simultaneously determine the kinetics and thermodynamics of chaperone−substrate interactions (*79*).

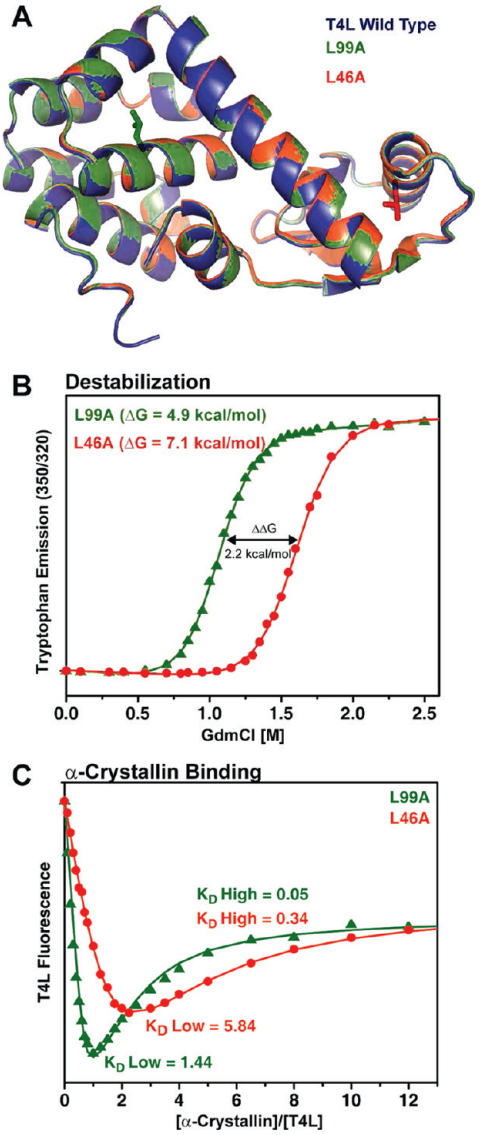

FIGURE 4: Destabilized model substrate for Hsp binding analysis. (A) Structural superimposition of cysteine-less pseudo-wild-type T4L (blue) and destabilized mutants L99A (green) and L46A (red) demonstrating preservation of tertiary structure. (B) Chemical denaturant unfolding curves of L99A and L46A as monitored by intrinsic tryptophan fluorescence depicting the relative destabilization of the two substrate mutations. (T4L WT ΔG = 11.3 kcal/mol). (C) Binding isotherms demonstrating that the affinity of α-crystallin for destabilized T4L mutants is reflective of relative destabilization. The left shift of the L99A curve demonstrates higher-affinity binding. K_D values of both low- and high-affinity substrate binding modes are reported adjacent to features of the binding isotherm corresponding to each mode.

A conceptual framework emerged from studies of T4L binding to sHSP that also incorporates previously reported mechanistic elements (*54*, *74*, *80*). It is grounded in experiments that identify the conformational states recognized by sHSP, define the nature of the chaperone structural changes that are required for or accompany recognition and binding, and determine binding affinity and stoichiometry. The resulting minimalist model is summarized by three coupled equilibria (Scheme 1). The substrate folding equilibrium (eq 1) describes the transition among the substrate native, partially unfolded,

and unfolded states. Equation 2 reflects the equilibrium associated with the transition of sHSP to a high-affinity and/or high-capacity state [$(sHSP)_a$]. This phenomenological description captures reported experimental characteristics of sHSP chaperone activity but simplifies the underlying distribution of oligomeric states and their relative affinities for non-native proteins. A more complete description should allow for low-affinity substrate binding by inactivated sHSP. Equations 1 and 2 are coupled by the binding of $(sHSP)_a$ to partially (I) or globally unfolded (U) states of the substrate (eq 3). Under steady-state conditions, the binding reflects an energetic preference of the non-native substrate states to associate with chaperones versus refolding to the native state N. The model predicts mutations or age-related substrate modifications that shift the equilibrium of eq 1 toward non-native states should induce formation of an sHSP complex. Similarly, the coupled equations predict that changes in the equilibrium of eq 2 favoring the activated state of the chaperone lead to an increased level of binding. The interpretive and predictive power of this model was tested in series of studies.

SHSP as stability sensors. Experiments confirm that manipulation of eq 1 affects the level of bound substrate (eq 3) as predicted. The affinity of binding of αA- and αB-crystallin, Hsp27 (*54*, *74*, *81*), and Hsp16.5 to T4L destabilized mutants correlates with the mutant's ΔG_{unf}. This is a remarkable result considering that these mutants have similar structures in the folded state with no local static unfolding, as demonstrated by X-ray crystallography (Figure 4A). Binding occurs in two modes with different affinities and stoichiometries (Figure 4C). The most destabilized T4L mutants activate a low-affinity but high-capacity mode whereby each sHSP subunit binds a monomer of T4L. By comparison, in the high-affinity mode, an average of four sHSP subunits bind a monomer of T4L. The two-state nature of the T4L folding equilibrium implies sHSP recognize the unfolded state, U, and/or partially unfolded intermediates whose populations increase with a decrease in ΔG_{unf}. Because binding occurs under conditions that strongly favor the folded state, the threshold for stable binding reflects the free energy balance between association with the sHSP and refolding to the native state. Consequently, in a set of mutants of similar native-state structures, sHSP sense the reduction in the stability of the native state.

Structure of the bound substrate. The reported spectrum of bound conformations appears to be substrate-specific and ranges from unfolded to loosely collapsed or molten globular (*82*−*88*). For instance, β- and γ-crystallins bound to α-crystallin were reported to have significant secondary structure, while an early report on α-lactalbumin binding suggests extensive unfolding. Although it is conceivable these differences may reflect the substrate-specific folding pathways, another contributing factor may be the intrinsic difficulty in the structural analysis of heterogeneous chaperone−substrate complexes. Heterogeneity is accentuated in aggregation-based assays where binding is induced by global substrate unfolding and determined by kinetics as discussed above. The possibility that the substrate intermediate recognized by

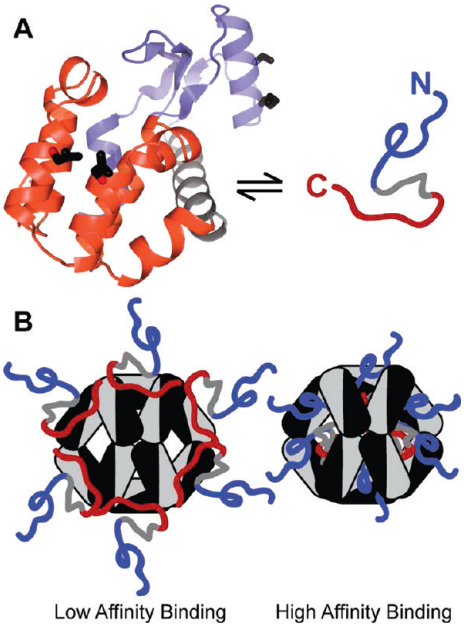

FIGURE 5: Structure of bound substrate and binding modes. (A) Crystal structure of T4L-L99A depicting representative residue pairs within the C-terminal domain (red) labeled to probe the tertiary fold and in the N-terminal region (blue) monitoring helical secondary structure proximities at i, $i + 4$ residues shown in equilibrium with a schematic representation of an unfolded form. (B) Model depicting structural aspects of the low- and high-affinity binding modes. In each case, there is extensive substrate unfolding with loss of proximities in labeled pairs tracking both secondary and tertiary structure. Labeled substrates report a net orientation with C-termini located in a more conformationally restrictive, solvent inaccessible environment and N-termini experiencing greater conformational mobility and solvent accessibility. The hydrodynamic radius of the high-affinity binding mode is comparable to that of the chaperone in the absence of substrate, and this radius increases under conditions favoring low-affinity binding.

sHSP differs substantially from the stably bound conformation due to subsequent rearrangements further confounds comparison of these studies. To overcome some of these issues, Claxton et al. carried out a systematic analysis of T4L structure when T4L is bound to α-crystallin under steady-state conditions in the absence of T4L aggregation (*84*). They monitored proximities of residue pairs that fingerprint the tertiary fold and secondary structures of T4L (Figure 5A). Binding to α-crystallin increases inter-residue distances within each domain as well as across the active site interface, suggesting a loss of T4L native structure. More importantly, an increase in the characteristic i, $i + 4$ helical distances implies extensive unfolding of bound T4L. Similar extensive unfolding was deduced for βB1-crystallin where binding to α-crystallin disrupts the dimer interface (*89*, *90*). In the context of the thermodynamic stability sensor model discussed above, a compelling interpretation of these results is that α-crystallin binds unfolded T4L. In contrast, a systematic study monitoring hydrogen−deuterium exchange reports limited protection of malate dehydrogenase (MDH) bound to Hsp16.9 (*87*). This suggests that either the bound conformation is partially folded or specific regions of unfolded MDH are protected in the chaperone complex. The lack of any significant changes in the Hsp16.9 protection by MDH binding led the authors to favor the second interpretation.

Understanding the origin of the differences in bound-substrate structures is critical for refining a mechanistic model of sHSP chaperone activity.

In the complex with α-crystallin, the hydrophobic C-terminus of T4L is predominantly buried in a low-dielectric/low-accessibility region, while regions of the N-terminal domain have increased backbone dynamics and are water-exposed (Figure 5B) (*84*). Long stretches of residues in the N-terminal domain possess flexibility characteristics of unfolded proteins in a sterically unhindered environment. The asymmetric pattern of contact suggests a preferential interaction of the sHSP with hydrophobic residues, considered a universal motif in substrate recognition by chaperones.

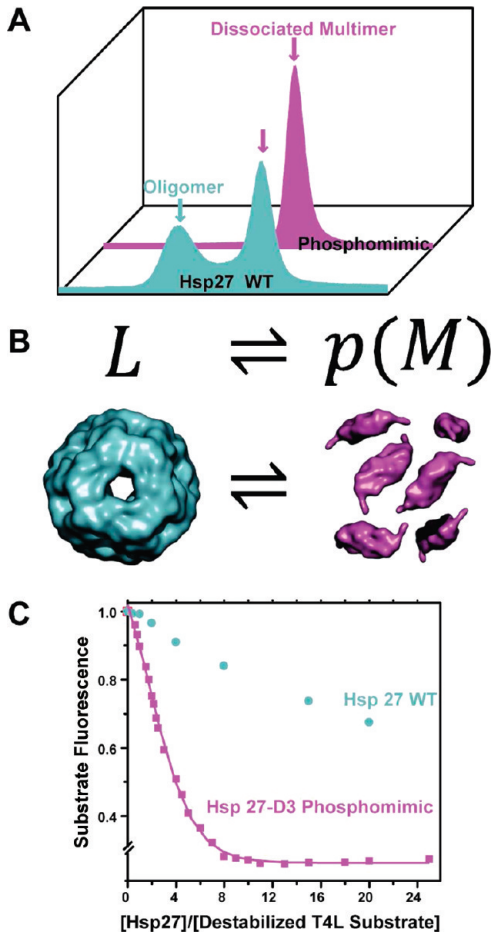

FIGURE 6: Hsp dissociation promotes activation and substrate binding. (A) Size-exclusion chromatography elution profiles of wild-type Hsp27 and a phosphorylation mimic in which the three serines phosphorylated by MAPK2 are replaced by aspartic acids to resemble this triply phosphorylated form (S15D/S78D/S82D). This phosphomimic shifts the oligomerization equilibrium in a manner favoring the complete disassembly of higher-order oligomers observed in WT Hsp27 to smaller species. (B) The equation represents the dissociation of Hsp27 from a large oligomer (L) to a multimer (M), where *p* is an integer that accounts for the difference in the number of subunits between the two oligomeric states. Below, this equilibrium is depicted graphically in colors corresponding to the predominant SEC peaks in panel A as well as the binding isotherms in panel C. (C) Binding is detected as quenching of a fluorescently labeled T4 lysozyme substrate. Phosphorylation-induced dissociation of Hsp27-D3 drastically increases the affinity of Hsp27 for substrate compared to that of WT Hsp27. Combined with panel A, these data reinforce a model of chaperone activation and regulation through phosphorylation-induced changes in the oligomeric state.

Role of oligomeric assembly in recognition and binding. Substrate contact regions have been identified in the N-terminal segment as well as in the α-crystallin domain of sHSP (*68*, *72*, *91*−*94*). Neither region is readily accessible in the native oligomer, suggesting that substrate binding requires substantial structural rearrangement. The conserved architecture of sHSP places the N-terminal domain in the core of the oligomer surrounded by an α-crystallin shell. Substrate access can be achieved either by expansion of the oligomer as observed for Hsp16.5-P1 (*70*) or through equilibrium dissociation (*47*, *51*, *54*). The notion of sHSP activation by dissociation was originally invoked to explain the increase in chaperone efficiency at higher temperatures (*49*, *53*, *95*−*98*). A dynamic threshold for function, mediated by increased rate constant of dissociation, was postulated to describe chaperone efficiency enhancement of α-crystallin mutants (*49*). Together, these observations suggest that the oligomer architecture serves as a switch that could be activated by stress signals. By regulating access to the substrate binding regions, the oligomer, with its complex symmetry and order, controls the sHSP apparent affinity and capacity and protects it from aberrant interactions with folded proteins.

In the context of this model, equilibrium dissociation allows sHSP to sense the presence of non-native proteins and dynamically respond to shifts in cellular folding equilibria. Modulation of the equilibrium appears to be central for the physiological roles of mammalian sHSP (*99*−*101*). αB-Crystallin and Hsp27 are phosphorylated in the context of cellular transduction pathways linked to growth, differentiation, and programmed cell death. Hsp27 phosphorylation at three serines leads to complete dissociation into a small multimer (*101*−*103*), presumably a dimer. Alterations in the equilibrium between various suboligomers were also reported as a consequence of αB-crystallin phosphorylation (*104*).

The role of equilibrium dissociation in regulating sHSP affinity was systematically tested by correlation of Hsp27 oligomeric state to T4L binding (*54*). In contrast to that of αA- and αB-crystallin, dissociation of Hsp27 into discrete small multimers (dimers) can be conveniently monitored by size-exclusion chromatography (Figure 6A,B). Perturbation of Hsp27 oligomer equilibrium by phosphorylation mimicking mutations that alter the relative stability of the two major oligomeric states profoundly affects the affinity and level of T4L binding. The mutations substantially increase T4L binding affinity and activate the high-capacity mode (Figure 6C). Conversely, mutations of Hsp27 or its phosphorylation mimic that reverse the dissociation, i.e., stabilize the native large oligomer, reduce but do not eliminate T4L binding levels, suggesting that the small multimer is the binding-competent species. T4L binding induces reassembly into Hsp27−T4L complexes with different hydrodynamic properties: those arising from low-affinity binding are larger, consistent with the higher capacity of this mode (*54*). In addition to establishing a direct link between dissociation and affinity, these results demonstrate that phosphorylation is an activation mechanism for Hsp27 and αB-crystallin.

There is evidence that the activation of some sHSP may occur without dissociation (*18*). Such a mechanism may be particularly relevant for monodisperse and symmetric

sHSP where there is no definitive evidence of equilibrium dissociation. Studies of yeast Hsp26 suggest a mechanistic decoupling between subunit exchange and chaperone activity. (*105*, *106*). In the absence of directly measuring binding affinities, it is impossible to unequivocally evaluate the contribution of native oligomer binding. Hsp16.5-P1 provides a structural framework for dissociation-independent activation where an increase in the size of the outer shell opening allows increased access to substrate binding regions (*70*). The extent to which sHSP from lower organisms utilize this proposed mechanism is yet to be fully explored.

IMPLICATIONS OF THE MODEL FOR UNDERSTANDING THE ROLE OF SHSP IN HEALTH AND DISEASE

This review presents an integrated structural and functional model of sHSP. Its central elements link sHSP affinity to oligomer structural dynamics and the free energy of substrate unfolding. Given the substantial binding capacity of sHSP, dynamic regulation of their affinity is critical for the cellular response to stress and aging. A static, low affinity may allow damaged proteins with marginal stability to "hang around" long enough to aggregate and precipitate. The exhaustion of α-crystallin from the water-soluble fraction of lens cells is a marker of age-related nuclear cataracts (*107*). On the other hand, a static high affinity may promote substrate unfolding based on the coupled thermodynamic model (Scheme 1). The buffering capacity of sHSP will be titrated out, clogging the chaperone network and the degradation machinery. This extreme case of a chaperone "gone awry" may be at the origin of the deleterious effects of some congenital cataract mutations in αA- and αB-crystallin (*25*, *27*). The αA-crystallin mutants, αA-R49C and αA-R116C, linked to hereditary cataracts have been shown to alter the affinity for T4L by orders of magnitude and increase the effective number of binding sites compared to that of WT (*80*). The enhanced binding by the αA-crystallin mutants shifts the substrate folding equilibrium toward non-native intermediates, thereby promoting unfolding of otherwise fully functional proteins (eqs 1−3). Given the high concentration of αA-crystallin in the lens, the implied molecular basis of cataracts is a gain of function that leads to the binding of undamaged proteins and subsequent precipitation of the saturated α-crystallin complexes in the developing lens of affected individuals.

Despite remarkable advances in understanding the mechanism of sHSP chaperone activity, much remains to be discovered regarding their physiological and biochemical functions. The eleven human sHSP appear to have important roles in signaling pathways, and we are just beginning to frame their contributions to health and disease. Emerging animal models, ex vivo tools, and cell culture systems promise to bridge the gap between the test tube and the organism for our understanding of the contribution of sHSP to physiological and pathological states.

ACKNOWLEDGMENT

We thank Derek P. Claxton and Dr. Hanane A. Koteiche for discussion and critical reading of the manuscript.

REFERENCES

1. Dill, K. A., and Chan, H. S. (1997) From Levinthal to pathways to funnels. *Nat. Struct. Biol. 4*, 10–19.
2. Onuchic, J. N., Luthey-Schulten, Z., and Wolynes, P. G. (1997) Theory of protein folding: The energy landscape perspective. *Annu. Rev. Phys. Chem. 48*, 545–600.
3. Dobson, C. M. (2004) Principles of protein folding, misfolding and aggregation. *Semin. Cell Dev. Biol. 15*, 3–16.
4. Bai, Y., Sosnick, T. R., Mayne, L., and Englander, S. W. (1995) Protein folding intermediates: Native-state hydrogen exchange. *Science 269*, 192–197.
5. Englander, S. W., Mayne, L., and Krishna, M. M. G. (2007) Protein folding and misfolding: Mechanism and principles. *Q. Rev. Biophys. 40*, 287–326.
6. Chiti, F., and Dobson, C. M. (2006) Protein misfolding, functional amyloid, and human disease. *Annu. Rev. Biochem. 75*, 333–366.
7. Bukau, B., Weissman, J., and Horwich, A. (2006) Molecular chaperones and protein quality control. *Cell 125*, 443–451.
8. Deuerling, E., and Bukau, B. (2004) Chaperone-assisted folding of newly synthesized proteins in the cytosol. *Crit. Rev. Biochem. Mol. Biol. 39*, 261–277.
9. Grantcharova, V., Alm, E. J., Baker, D., and Horwich, A. L. (2001) Mechanisms of protein folding. *Curr. Opin. Struct. Biol. 11*, 70–82.
10. Horwich, A. L., Fenton, W. A., and Rapoport, T. A. (2001) Protein folding taking shape. Workshop on molecular chaperones. *EMBO Rep. 2*, 1068–1073.
11. Lin, Z., and Rye, H. S. (2006) GroEL-mediated protein folding: Making the impossible, possible. *Crit. Rev. Biochem. Mol. Biol. 41*, 211–239.
12. Mogk, A., and Bukau, B. (2004) Molecular chaperones: Structure of a protein disaggregase. *Curr. Biol. 14*, R78–R80.
13. Naylor, D. J., and Hartl, F. U. (2001) Contribution of molecular chaperones to protein folding in the cytoplasm of prokaryotic and eukaryotic cells. *Biochem. Soc. Symp.*, 45–68.
14. Parsell, D. A., and Lindquist, S. (1993) The function of heat-shock proteins in stress tolerance: Degradation and reactivation of damaged proteins. *Annu. Rev. Genet. 27*, 437–496.
15. Xu, Z., and Sigler, P. B. (1998) GroEL/GroES: Structure and function of a two-stroke folding machine. *J. Struct. Biol. 124*, 129–141.
16. Caspers, G. J., Leunissen, J. A., and de Jong, W. W. (1995) The expanding small heat-shock protein family, and structure predictions of the conserved "α-crystallin domain". *J. Mol. Evol. 40*, 238–248.
17. de Jong, W. W., Caspers, G. J., and Leunissen, J. A. (1998) Genealogy of the α-crystallin−small heat-shock protein superfamily. *Int. J. Biol. Macromol. 22*, 151–162.
18. Haslbeck, M., Franzmann, T., Weinfurtner, D., and Buchner, J. (2005) Some like it hot: The structure and function of small heat-shock proteins. *Nat. Struct. Mol. Biol. 12*, 842–846.
19. Van Montfort, R., Slingsby, C., and Vierling, E. (2001) Structure and function of the small heat shock protein/α-crystallin family of molecular chaperones. *Adv. Protein Chem. 59*, 105–156.
20. Haley, D. A., Bova, M. P., Huang, Q. L., Mchaourab, H. S., and Stewart, P. L. (2000) Small heat-shock protein structures reveal a continuum from symmetric to variable assemblies. *J. Mol. Biol. 298*, 261–272.
21. Hsu, A. L., Murphy, C. T., and Kenyon, C. (2003) Regulation of aging and age-related disease by DAF-16 and heat-shock factor. *Science. 300*, 1142–1145 [Erratum, (2003) *Science 300*, 2033].
22. Arrigo, A.-P., Paul, C., Ducasse, C., Manero, F., Kretz-Remy, C., Virot, S., Javouhey, E., Mounier, N., and Diaz-Latoud, C. (2002) Small stress proteins: Novel negative modulators of apoptosis induced independently of reactive oxygen species. *Prog. Mol. Subcell. Biol. 28*, 185–204.
23. Bruey, J. M., Ducasse, C., Bonniaud, P., Ravagnan, L., Susin, S. A., Diaz-Latoud, C., Gurbuxani, S., Arrigo, A. P., Kroemer, G., Solary, E., and Garrido, C. (2000) Hsp27 negatively regulates cell death by interacting with cytochrome c. *Nat. Cell Biol. 2*, 645–652.
24. Samali, A., Robertson, J. D., Peterson, E., Manero, F., van Zeijl, L., Paul, C., Cotgreave, I. A., Arrigo, A. P., and Orrenius, S. (2001) Hsp27 protects mitochondria of thermotolerant cells against apoptotic stimuli. *Cell Stress Chaperones 6*, 49–58.
25. Litt, M., Kramer, P., LaMorticella, D. M., Murphey, W., Lovrien, E. W., and Weleber, R. G. (1998) Autosomal dominant congenital cataract associated with a missense mutation in the human α crystallin gene CRYAA. *Hum. Mol. Genet. 7*, 471–474.
26. Mackay, D., Andley, U., and Shiels, A. (2003) Cell death triggered by a novel mutation in the αA-crystallin gene underlies autosomal

dominant cataract linked to chromosome 21q. *Eur. J. Hum. Genet. 11*, 784–793.
27. Vicart, P., Caron, A., Guicheney, P., Li, Z., Prevost, M. C., Faure, A., Chateau, D., Chapon, F., Tome, F., Dupret, J. M., Paulin, D., and Fardeau, M. (1998) A missense mutation in the αB-crystallin chaperone gene causes a desmin-related myopathy. *Nat. Genet. 20*, 92–95.
28. Ousman, S. S., Tomooka, B. H., van Noort, J. M., Wawrousek, E. F., O'Connor, K. C., Hafler, D. A., Sobel, R. A., Robinson, W. H., and Steinman, L. (2007) Protective and therapeutic role for αB-crystallin in autoimmune demyelination. *Nature 448*, 474–479.
29. Sharp, P. S., Akbar, M. T., Bouri, S., Senda, A., Joshi, K., Chen, H. J., Latchman, D. S., Wells, D. J., and de Belleroche, J. (2008) Protective effects of heat shock protein 27 in a model of ALS occur in the early stages of disease progression. *Neurobiol. Dis. 30*, 42–55.
30. Arrigo, A.-P., Simon, S., Gibert, B., Kretz-Remy, C., Nivon, M., Czekalla, A., Guillet, D., Moulin, M., Diaz-Latoud, C., and Vicart, P. (2007) Hsp27 (HspB1) and αB-crystallin (HspB5) as therapeutic targets. *FEBS Lett. 581*, 3665–3674.
31. McLemore, E. C., Tessier, D. J., Thresher, J., Komalavilas, P., and Brophy, C. M. (2005) Role of the small heat shock proteins in regulating vascular smooth muscle tone. *J. Am. Coll. Surg. 201*, 30–36.
32. Horwitz, J. (1993) Proctor Lecture. The function of α-crystallin. *Invest. Ophthalmol. Visual Sci. 34*, 10–22.
33. Bloemendal, H., de Jong, W., Jaenicke, R., Lubsen, N. H., Slingsby, C., and Tardieu, A. (2004) Ageing and vision: Structure, stability and function of lens crystallins. *Prog. Biophys. Mol. Biol. 86*, 407–485.
34. Lampi, K. J., Shih, M., Ueda, Y., Shearer, T. R., and David, L. L. (2002) Lens proteomics: Analysis of rat crystallin sequences and two-dimensional electrophoresis map. *Invest. Ophthalmol. Visual Sci. 43*, 216–224.
35. Ueda, Y., Duncan, M. K., and David, L. L. (2002) Lens proteomics: The accumulation of crystallin modifications in the mouse lens with age. *Invest. Ophthalmol. Visual Sci. 43*, 205–215.
36. Truscott, R. J. W. (2005) Age-related nuclear cataract-oxidation is the key. *Exp. Eye Res. 80*, 709–725.
37. Horwitz, J. (2000) The function of α-crystallin in vision. *Semin. Cell Dev. Biol. 11*, 53–60.
38. Horwitz, J., Emmons, T., and Takemoto, L. (1992) The ability of lens α-crystallin to protect against heat-induced aggregation is age-dependent. *Curr. Eye Res. 11*, 817–822.
39. Brady, J. P., Garland, D., Duglas-Tabor, Y., Robison, W. G.Jr., Groome, A., and Wawrousek, E. F. (1997) Targeted disruption of the mouse αA-crystallin gene induces cataract and cytoplasmic inclusion bodies containing the small heat shock protein αB-crystallin. *Proc. Natl. Acad. Sci. U.S.A. 94*, 884–889.
40. Chang, B., Hawes, N. L., Roderick, T. H., Smith, R. S., Heckenlively, J. R., Horwitz, J., and Davisson, M. T. (1999) Identification of a missense mutation in the αA-crystallin gene of the lop18 mouse. *Mol. Vision 5*, 21.
41. Graw, J., Loster, J., Soewarto, D., Fuchs, H., Meyer, B., Reis, A., Wolf, E., Balling, R., and Hrabe de Angelis, M. (2001) Characterization of a new, dominant V124E mutation in the mouse αA-crystallin-encoding gene. *Invest. Ophthalmol. Visual Sci. 42*, 2909–2915.
42. Andley, U. P. (2007) Crystallins in the eye: Function and pathology. *Prog. Retinal Eye Res. 26*, 78–98.
43. Hsu, C.-D., Kymes, S., and Petrash, J. M. (2006) A transgenic mouse model for human autosomal dominant cataract. *Invest. Ophthalmol. Visual Sci. 47*, 2036–2044.
44. Kim, K. K., Kim, R., and Kim, S. H. (1998) Crystal structure of a small heat-shock protein. *Nature 394*, 595–599.
45. Bova, M. P., Mchaourab, H. S., Han, Y., and Fung, B. K. (2000) Subunit exchange of small heat shock proteins. Analysis of oligomer formation of αA-crystallin and Hsp27 by fluorescence resonance energy transfer and site-directed truncations. *J. Biol. Chem. 275*, 1035–1042.
46. Haley, D. A., Horwitz, J., and Stewart, P. L. (1998) The small heat-shock protein, αB-crystallin, has a variable quaternary structure. *J. Mol. Biol. 277*, 27–35.
47. van Montfort, R. L., Basha, E., Friedrich, K. L., Slingsby, C., and Vierling, E. (2001) Crystal structure and assembly of a eukaryotic small heat shock protein. *Nat. Struct. Biol. 8*, 1025–1030.
48. Bova, M. P., Huang, Q., Ding, L., and Horwitz, J. (2002) Subunit exchange, conformational stability, and chaperone-like function of the small heat shock protein 16.5 from *Methanococcus jannaschii*. *J. Biol. Chem. 277*, 38468–38475.
49. Koteiche, H. A., Berengian, A. R., and Mchaourab, H. S. (1998) Identification of protein folding patterns using site-directed spin labeling. Structural characterization of a β-sheet and putative substrate binding regions in the conserved domain of αA-crystallin. *Biochemistry 37*, 12681–12688.
50. Ehrnsperger, M., Lilie, H., Gaestel, M., and Buchner, J. (1999) The dynamics of Hsp25 quaternary structure. Structure and function of different oligomeric species. *J. Biol. Chem. 274*, 14867–14874.
51. Giese, K. C., and Vierling, E. (2002) Changes in oligomerization are essential for the chaperone activity of a small heat shock protein in vivo and in vitro. *J. Biol. Chem. 277*, 46310–46318.
52. Giese, K. C., and Vierling, E. (2004) Mutants in a small heat shock protein that affect the oligomeric state. Analysis and allele-specific suppression. *J. Biol. Chem. 279*, 32674–32683.
53. Haslbeck, M., Walke, S., Stromer, T., Ehrnsperger, M., White, H. E., Chen, S., Saibil, H. R., and Buchner, J. (1999) Hsp26: A temperature-regulated chaperone. *EMBO J. 18*, 6744–6751.
54. Shashidharamurthy, R., Koteiche, H. A., Dong, J.and McHaourab, H. S.(2005) Mechanism of chaperone function in small heat shock proteins: Dissociation of the HSP27 oligomer is required for recognition and binding of destabilized T4 lysozyme. *J. Biol. Chem. 280*, 5281–5289.
55. Koteiche, H. A., and Mchaourab, H. S. (1999) Folding pattern of the α-crystallin domain in αA-crystallin determined by site-directed spin labeling. *J. Mol. Biol. 294*, 561–577.
56. Berengian, A. R., Bova, M. P., and Mchaourab, H. S. (1997) Structure and function of the conserved domain in αA-crystallin. Site-directed spin labeling identifies a β-strand located near a subunit interface. *Biochemistry 36*, 9951–9957.
57. Berengian, A. R., Parfenova, M., and Mchaourab, H. S. (1999) Site-directed spin labeling study of subunit interactions in the α-crystallin domain of small heat-shock proteins. Comparison of the oligomer symmetry in αA-crystallin, HSP 27, and HSP 16.3. *J. Biol. Chem. 274*, 6305–6314.
58. Mchaourab, H. S., Berengian, A. R., and Koteiche, H. A. (1997) Site-directed spin-labeling study of the structure and subunit interactions along a conserved sequence in the α-crystallin domain of heat-shock protein 27. Evidence of a conserved subunit interface. *Biochemistry 36*, 14627–14634.
59. Feil, I. K., Malfois, M., Hendle, J., van Der Zandt, H., and Svergun, D. I. (2001) A novel quaternary structure of the dimeric α-crystallin domain with chaperone-like activity. *J. Biol. Chem. 276*, 12024–12029.
60. Jehle, S., van Rossum, B., Stout, J. R., Noguchi, S. M., Falber, K., Rehbein, K., Oschkinat, H., Klevit, R. E., and Rajagopal, P. (2009) αB-Crystallin: A hybrid solid-state/solution-state NMR investigation reveals structural aspects of the heterogeneous oligomer. *J. Mol. Biol. 385*, 1481–1497.
61. Kennaway, C. K., Benesch, J. L., Gohlke, U., Wang, L., Robinson, C. V., Orlova, E. V., Saibil, H. R., and Keep, N. H. (2005) Dodecameric structure of the small heat shock protein Acr1 from *Mycobacterium tuberculosis*. *J. Biol. Chem. 280*, 33419–33425 [Erratum, (2005) *J. Biol. Chem. 280*, 38888].
62. Koteiche, H. A., and McHaourab, H. S. (2002) The determinants of the oligomeric structure in Hsp16.5 are encoded in the α-crystallin domain. *FEBS Lett. 519*, 16–22.
63. Aquilina, J. A., Benesch, J. L. P., Bateman, O. A., Slingsby, C., and Robinson, C. V. (2003) Polydispersity of a mammalian chaperone: Mass spectrometry reveals the population of oligomers in αB-crystallin. *Proc. Natl. Acad. Sci. U.S.A. 100*, 10611–10616.
64. Bova, M. P., Horwitz, J., and Fung, B. K. (1997) Subunit exchange of αA-crystallin. *J. Biol. Chem. 272*, 29511–29517.
65. White, H. E., Orlova, E. V., Chen, S., Wang, L., Ignatiou, A., Gowen, B., Stromer, T., Franzmann, T. M., Haslbeck, M., Buchner, J., and Saibil, H. R. (2006) Multiple distinct assemblies reveal conformational flexibility in the small heat shock protein Hsp26. *Structure 14*, 1197–1204.
66. Merck, K. B., Horwitz, J., Kersten, M., Overkamp, P., Gaestel, M., Bloemendal, H., and de Jong, W. W. (1993) Comparison of the homologous carboxy-terminal domain and tail of α-crystallin and small heat shock protein. *Mol. Biol. Rep. 18*, 209–215.
67. Merck, K. B., Groenen, P. J., Voorter, C. E., de Haard-Hoekman, W. A., Horwitz, J., Bloemendal, H., and de Jong, W. W. (1993) Structural and functional similarities of bovine α-crystallin and mouse small heat-shock protein. A family of chaperones. *J. Biol. Chem. 268*, 1046–1052.
68. Stromer, T., Fischer, E., Richter, K., Haslbeck, M., and Buchner, J. (2004) Analysis of the regulation of the molecular chaperone Hsp26

by temperature-induced dissociation: The N-terminal domail is important for oligomer assembly and the binding of unfolding proteins. *J. Biol. Chem. 279*, 11222–11228.
69. Sobott, F., Benesch, J. L., Vierling, E., and Robinson, C. V. (2002) Subunit exchange of multimeric protein complexes. Real-time monitoring of subunit exchange between small heat shock proteins by using electrospray mass spectrometry. *J. Biol. Chem. 277*, 38921–38929.
70. Shi, J., Koteiche, H. A., McHaourab, H. S., and Stewart, P. L. (2006) Cryoelectron microscopy and EPR analysis of engineered symmetric and polydisperse Hsp16.5 assemblies reveals determinants of polydispersity and substrate binding. *J. Biol. Chem. 281*, 40420–40428.
71. Ehrnsperger, M., Graber, S., Gaestel, M., and Buchner, J. (1997) Binding of non-native protein to Hsp25 during heat shock creates a reservoir of folding intermediates for reactivation. *EMBO J. 16*, 221–229.
72. Lee, G. J., Roseman, A. M., Saibil, H. R., and Vierling, E. (1997) A small heat shock protein stably binds heat-denatured model substrates and can maintain a substrate in a folding-competent state. *EMBO J. 16*, 659–671.
73. Gidalevitz, T., Ben-Zvi, A., Ho, K. H., Brignull, H. R., and Morimoto, R. I. (2006) Progressive disruption of cellular protein folding in models of polyglutamine diseases. *Science 311*, 1471–1474.
74. Mchaourab, H. S., Dodson, E. K., and Koteiche, H. A. (2002) Mechanism of Chaperone Function in Small Heat-Shock Proteins. Two-Mode Binding of the Excited States of T4 Lysozyme Mutants by αA-Crystallin. *J. Biol. Chem. 277*, 40557–40566.
75. Matthews, B. W. (1995) Studies on protein stability with T4 lysozyme. *Adv. Protein Chem. 46*, 249–278.
76. Matthews, B. W. (1996) Structural and genetic analysis of the folding and function of T4 lysozyme. *FASEB J. 10*, 35–41.
77. Sathish, H. A., Koteiche, H. A., and McHaourab, H. S. (2004) Binding of destabilized βB2-crystallin mutants to α-crystallin: The role of a folding intermediate. *J. Biol. Chem. 279*, 16425–16432.
78. Sathish, H. A., Stein, R. A., Yang, G., and Mchaourab, H. S. (2003) Mechanism of chaperone function in small heat-shock proteins. Fluorescence studies of the conformations of T4 lysozyme bound to αB-crystallin. *J. Biol. Chem. 278*, 44214–44221.
79. Latham, J. C., Stein, R. A., Bornhop, D. J., and McHaourab, H. S. (2009) Free-Solution Label-Free Detection of α-Crystallin Chaperone Interactions by Back-Scattering Interferometry. *Anal. Chem. 81*, 1865–1871.
80. Koteiche, H. A., and McHaourab, H. S. (2006) Mechanism of a Hereditary Cataract Phenotype: Mutations in αA-crystallin activate substrate binding. *J. Biol. Chem. 281*, 14273–14279.
81. Koteiche, H. A., and McHaourab, H. S. (2003) Mechanism of chaperone function in small heat-shock proteins. Phosphorylation-induced activation of two-mode binding in αB-crystallin. *J. Biol. Chem. 278*, 10361–10367.
82. Bettelheim, F. A., Ansari, R., Cheng, Q. F., and Zigler, J. S.Jr. (1999) The mode of chaperoning of dithiothreitol-denatured α-lactalbumin by α-crystallin. *Biochem. Biophys. Res. Commun. 261*, 292–297.
83. Carver, J. A., Lindner, R. A., Lyon, C., Canet, D., Hernandez, H., Dobson, C. M., and Redfield, C. (2002) The interaction of the molecular chaperone α-crystallin with unfolding α-lactalbumin: A structural and kinetic spectroscopic study. *J. Mol. Biol. 318*, 815–827.
84. Claxton, D. P., Zou, P., and McHaourab, H. S. (2008) Structure and orientation of T4 lysozyme bound to the small heat shock protein α-crystallin. *J. Mol. Biol. 375*, 1026–1039.
85. Das, K. P., Choo-Smith, L. P., Petrash, J. M., and Surewicz, W. K. (1999) Insight into the secondary structure of non-native proteins bound to a molecular chaperone α-crystallin. An isotope-edited infrared spectroscopic study. *J. Biol. Chem. 274*, 33209–33212.
86. Das, K. P., Petrash, J. M., and Surewicz, W. K. (1996) Conformational properties of substrate proteins bound to a molecular chaperone α-crystallin. *J. Biol. Chem. 271*, 10449–10452.
87. Cheng, G., Basha, E., Wysocki, V. H., and Vierling, E. (2008) Insights into small heat shock protein and substrate structure during chaperone action derived from hydrogen/deuterium exchange and mass spectrometry. *J. Biol. Chem. 283*, 26634–26642.
88. Stromer, T., Ehrnsperger, M., Gaestel, M., and Buchner, J. (2003) Analysis of the interaction of small heat shock proteins with unfolding proteins. *J. Biol. Chem. 278*, 18015–18021.
89. Koteiche, H. A., Kumar, M. S., and Mchaourab, H. S. (2007) Analysis of βB1-crystallin unfolding equilibrium by spin and fluorescence labeling: Evidence of a dimeric intermediate. *FEBS Lett. 581*, 1933–1938.
90. Mchaourab, H. S., Kumar, M. S., and Koteiche, H. A. (2007) Specificity of αA-crystallin binding to destabilized mutants of βB1-crystallin. *FEBS Lett. 581*, 1939–1943.
91. Sharma, K. K., Kaur, H., and Kester, K. (1997) Functional elements in molecular chaperone α-crystallin: Identification of binding sites in αB-crystallin. *Biochem. Biophys. Res. Commun. 239*, 217–222.
92. Sharma, K. K., Kumar, G. S., Murphy, A. S., and Kester, K. (1998) Identification of 1,1′-bi(4-anilino)naphthalene-5,5′-disulfonic acid binding sequences in α-crystallin. *J. Biol. Chem. 273*, 15474–15478.
93. Ghosh, J. G., Estrada, M. R., and Clark, J. I. (2005) Interactive domains for chaperone activity in the small heat shock protein, human αB crystallin. *Biochemistry 44*, 14854–14869.
94. Ghosh, J. G., Shenoy, A. K.Jr., and Clark, J. I. (2006) N- and C-Terminal motifs in human αB crystallin play an important role in the recognition, selection, and solubilization of substrates. *Biochemistry 45*, 13847–13854.
95. Das, B. K., Liang, J. J., and Chakrabarti, B. (1997) Heat-induced conformational change and increased chaperone activity of lens α-crystallin. *Curr. Eye Res. 16*, 303–309.
96. Das, K. P., and Surewicz, W. K. (1995) Temperature-induced exposure of hydrophobic surfaces and its effect on the chaperone activity of α-crystallin. *FEBS Lett. 369*, 321–325.
97. Lee, G. J., Pokala, N., and Vierling, E. (1995) Structure and in vitro molecular chaperone activity of cytosolic small heat shock proteins from pea. *J. Biol. Chem. 270*, 10432–10438.
98. Reddy, G. B., Das, K. P., Petrash, J. M., and Surewicz, W. K. (2000) Temperature-dependent chaperone activity and structural properties of human αA- and αB-crystallins. *J. Biol. Chem. 275*, 4565–4570.
99. Mehlen, P., Mehlen, A., Guillet, D., Preville, X., and Arrigo, A. P. (1995) Tumor necrosis factor-α induces changes in the phosphorylation, cellular localization, and oligomerization of human hsp27, a stress protein that confers cellular resistance to this cytokine. *J. Cell. Biochem. 58*, 248–259.
100. Morrison, L. E., Hoover, H. E., Thuerauf, D. J., and Glembotski, C. C. (2003) Mimicking phosphorylation of αB-crystallin on serine-59 is necessary and sufficient to provide maximal protection of cardiac myocytes from apoptosis. *Circ. Res. 92*, 203–211.
101. Rogalla, T., Ehrnsperger, M., Preville, X., Kotlyarov, A., Lutsch, G., Ducasse, C., Paul, C., Wieske, M., Arrigo, A. P., Buchner, J., and Gaestel, M. (1999) Regulation of Hsp27 oligomerization, chaperone function, and protective activity against oxidative stress/tumor necrosis factor α by phosphorylation. *J. Biol. Chem. 274*, 18947–18956.
102. Benndorf, R., Engel, K., and Gaestel, M. (2000) Analysis of small Hsp phosphorylation. *Methods Mol. Biol. 99*, 431–445.
103. Preville, X., Schultz, H., Knauf, U., Gaestel, M., and Arrigo, A. P. (1998) Analysis of the role of Hsp25 phosphorylation reveals the importance of the oligomerization state of this small heat shock protein in its protective function against TNFα- and hydrogen peroxide-induced cell death. *J. Cell. Biochem. 69*, 436–452.
104. Aquilina, J. A., Benesch, J. L., Ding, L. L., Yaron, O., Horwitz, J., and Robinson, C. V. (2004) Phosphorylation of αB-crystallin alters chaperone function through loss of dimeric substructure. *J. Biol. Chem. 279*, 28675–28680.
105. Franzmann, T. M., Menhorn, P., Walter, S., and Buchner, J. (2008) Activation of the chaperone Hsp26 is controlled by the rearrangement of its thermosensor domain. *Mol. Cell 29*, 207–216.
106. Franzmann, T. M., Wuhr, M., Richter, K., Walter, S., and Buchner, J. (2005) The activation mechanism of Hsp26 does not require dissociation of the oligomer. *J. Mol. Biol. 350*, 1083–1093.
107. Roy, D., and Spector, A. (1976) Absence of low-molecular-weight α crystallin in nuclear region of old human lenses. *Proc. Natl. Acad. Sci. U.S.A. 73*, 3484–3487.